

Removal of C_3F_8 Via the Combination of Non-Thermal Plasma, Adsorption and Catalysis

Bor Yuan Lin · Moo Been Chang · Hsin Liang Chen · How Ming Lee · Sheng Jen Yu · Shou Nan Li

Received: 20 September 2010 / Accepted: 11 May 2011 / Published online: 27 May 2011
© Springer Science+Business Media, LLC 2011

Abstract The feasibility of C_3F_8 abatement via combining nonthermal plasma with adsorption and/or catalysis is investigated in this study. In terms of the simultaneous combination of plasma, adsorption and catalysis (CPAC), three different configurations including A/C layer (adsorbent layer prior to catalyst layer), C/A layer (catalyst layer prior to adsorbent layer) and A/C mixture (adsorbent and catalyst are mechanically mixed) are adopted. For all the experimental tests conducted in this study, the gas stream consists of 500 ppm C_3F_8 , 2% O_2 , and balanced N_2 . The experimental results indicate that C_3F_8 removal efficiencies depend on what kind of packing material is adopted (adsorbent, catalyst or both) and how the material is packed within the plasma reactor. The removal efficiencies obtained with different reactors are in the order as: CPAC (A/C layer; AC mixture) > CPA (plasma with adsorbent alone) > CPC (plasma with catalyst alone) > CPAC (C/A layer). The identified products after treatment include CO_2 , CO, N_2O and CF_4 . The formation of C_2F_6 is not observed in this study, which is encouraging since the global warming potential of C_2F_6 is actually higher than that of C_3F_8 .

Keywords Global warming · Greenhouse gases (GHGs) · Perfluorocompounds (PFCs) · Plasma catalysis · Adsorbent

B. Y. Lin · M. B. Chang (✉)
Graduate Institute of Environmental Engineering, National Central University, Chung-Li, Taoyuan County 320, Taiwan, ROC
e-mail: mbchang@ncuen.ncu.edu.tw

H. L. Chen · H. M. Lee
Physics Division, Institute of Nuclear Energy Research (INER), Longtan, Taoyuan County 325, Taiwan, ROC

S. J. Yu · S. N. Li
Industrial Technology Research Institute (ITRI), Hsinchu 310, Taiwan, ROC

Introduction

With the characteristics of extremely long lifetimes in the atmosphere and relatively high GWPs (global warming potentials), PFCs are regulated as one of the GHGs (greenhouse gases) in Kyoto Protocol. PFCs are mainly emitted from semiconductor and TFT-LCD manufacturing industries. In terms of PFC abatement, the high temperature-based technologies including catalytic oxidation and thermal decomposition are still the mainstream. Although acceptable removal efficiency could be achieved, these equipments have to be maintained at a certain temperature even during the period without PFC emission. Different from the above-mentioned technologies, nonthermal plasma can be ignited and operated at room temperature, making it a potentially viable technique for PFC abatement. However, prior to further industrial application, the energy efficiency and the products' selectivities still need to be improved [1, 2].

To resolve these challenges, a novel technique combining the nonthermal plasma, adsorption and catalysis (CPAC) simultaneously is developed in this study. It has been experimentally demonstrated in various studies that introducing catalyst into a nonthermal plasma reactor could effectively improve the abatement of gaseous pollutants [3–9]. Moreover, adsorbent is used to increase the concentration and retention time of pollutant molecules within discharge region, which is believed to be beneficial for energy efficiency and products' selectivities. C_3F_8 is chosen as the target pollutant in this study because it has been gradually replacing CF_4 and C_2F_6 as the CVD chamber cleaning gas for semiconductor industry. The main purpose is to demonstrate the feasibility of PFC abatement via CPAC, which is constructed by introducing the same volumes of adsorbent and catalyst in the arrangements of two separate layers or a single layer (i.e. adsorbent and catalyst are mechanically mixed.). In addition to CPAC, the combinations of plasma with catalysis or adsorption alone, which are termed as CPC and CPA, are used as control as well.

Experimental

Physical Properties of the Catalyst and Adsorbents

The γ - Al_2O_3 and molecular sieves (MS-3A, MS-4A, MS-4A and MS-10A) pellets used as catalyst and adsorbent in this study are commercial products purchased from Alfa Aesae and Merck KGaA, respectively. The γ - Al_2O_3 and molecular sieve pellets are of spherical and cylindrical shape, respectively. To confirm the catalytic activity of γ - Al_2O_3 , α - Al_2O_3 pellets are prepared in laboratory by calcinating γ - Al_2O_3 in air at 1,200°C for 3 h. As shown in Fig. 1, the results of XRD analysis demonstrated calcination of γ - Al_2O_3 in air could obtain the α - Al_2O_3 needed for the experiment.

Nitrogen BET measurements were carried out for the materials applied. The results are listed in Table 1. For molecular sieves, the average pore diameter increased as the BET surface areas increased. For instance, the BET surface areas of MS-3A, MS-4A, MS-5A, and MS-10A are 22.50, 290.54, 370.86, and 456.56 m^2/g , and the average pore diameters of MS-3A, MS-4A, MS-5A, and MS-10A are 3.52, 4.32, 5.20, and 10.12 Å, respectively. For aluminum oxides, α - Al_2O_3 is nonporous while γ - Al_2O_3 is porous. Therefore, the BET surface area of α - Al_2O_3 was relatively small (c.a. 9.79 m^2/g) compared to that of γ - Al_2O_3 , and the average pore diameters of α - Al_2O_3 was not analyzed.

Fig. 1 XRD spectra of γ - Al_2O_3 and α - Al_2O_3 . The symbols “ α ” and “ γ ” represent crystalline α - Al_2O_3 and γ - Al_2O_3 , respectively

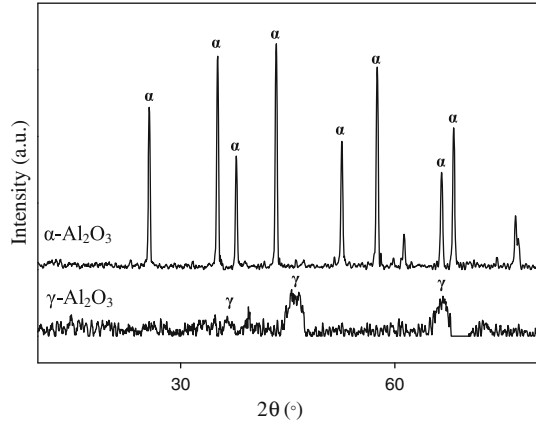


Table 1 BET surface area and average pore size of materials

Material	Shape	Size (mm)	BET surface area (m ² /g)	Average pore diameter (Å)
MS-3A	Sphere	2	22.50	3.52
MS-4A	Sphere	2	290.54	4.32
MS-5A	Sphere	2	370.86	5.20
MS-10A	Sphere	2	456.56	10.12
γ - Al_2O_3	Cylinder	D:3.2 L:4–5	249.33	7.14
α - Al_2O_3	Cylinder	D:3.2 L:4–5	9.79	n.a.

n.a. not analyzed

The symbols “D” and “L” represent the diameter and length, respectively

Experimental Tests of C_3F_8 Abatement

The laboratory-scale experimental system used to evaluate the effectiveness of C_3F_8 decomposition is schematically shown in Fig. 2. The experimental apparatus was comprised of a gas-generation system, high-voltage power supply system, a plasma reactor, and sampling detection system. The gas-generation system consisted of several gas cylinders, including $\text{C}_3\text{F}_8/\text{N}_2$, N_2 , and O_2 and was regulated by a set of mass flow meters (MKS-1179A) to control the flow rates of feeding gases. The composition of the gas streams could be accurately controlled by mass flow meters.

The high-voltage power supply system consists of a power meter (Chen-Hwa Co., Model 2100, Power-Win Technology) and a high-voltage transformer (Jui-Hsiang PTY Co. Ltd.). For all experiments carried out in this study, the applied frequency was fixed at 200 Hz and the applied voltage ranged from 12 to 18 kV (rms value). The discharge power was determined by the Lissajous diagram (V-Q plot) [10] which was measured by a digital oscilloscope (Tektronix 3014B) equipped with a high voltage probe (Tektronix P6015A) and a voltage probe (Tektronix 613B). A 10 μF capacitor was connected in series with the reactor for the measurement of the charge.

The laboratory-scale plasma reactor consisting of cylindrical tube, inner electrode, and outer electrode is schematically described in Fig. 3. The cylindrical tube was made of quartz with outer and inner diameters of 2.8 and 2.5 cm, respectively. The inner electrode

Fig. 2 Schematic diagram of the experimental set-up of single-stage system

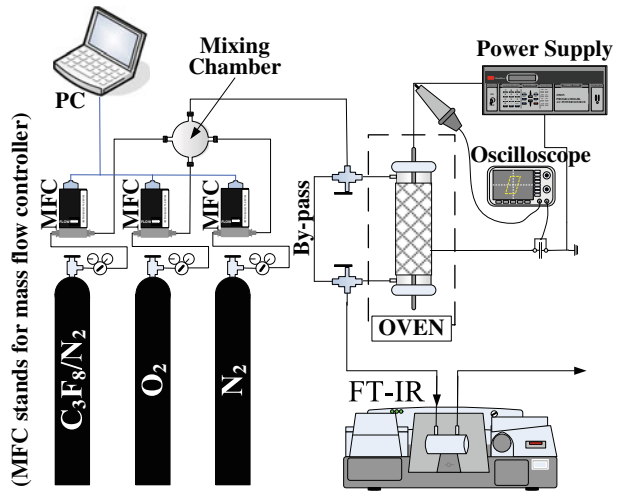
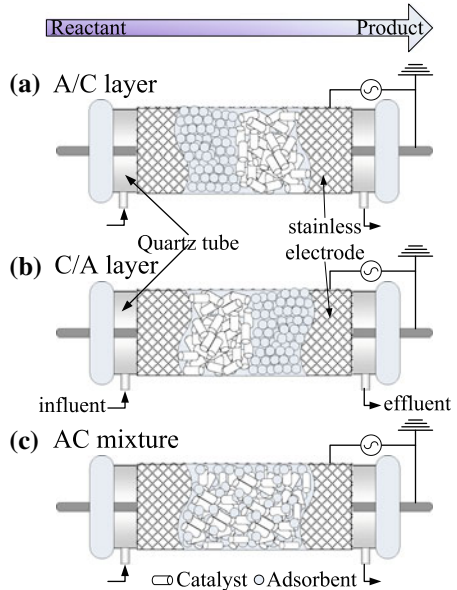


Fig. 3 Illustrations of the different CPACs tested in this study



was composed of a stainless steel rod (diameter, 0.3 cm) and was located along the tube's centerline. The outer electrode, made of stainless steel mesh, was wrapped around the outside of the crystal quartz tube. The discharge length is 10 cm. For the simultaneous combination of plasma, adsorption and catalysis, three different configurations are tested in this study, including A/C (adsorbent layer prior to catalyst layer), C/A (catalyst layer prior to adsorbent layer) and A/C mixture (adsorbent and catalyst are mechanically mixed). The experimental tests were conducted at different temperatures varying from room to high temperature (ca. 25–250°C) and gas streams were kept at ambient pressure in the plasma reactor for all tests. For all the experimental tests for C_3F_8 abatement by plasma (including CPC, CPA and CPAC), the gas stream consists of 500 ppm C_3F_8 , 2% O_2 , and balanced N_2 .

O₂ content is fixed at 2% because our experimental results show that C₃F₈ removal efficiency increases with O₂ content up to 2% but further increase in O₂ content would lead to a lower removal efficiency instead.

Qualitative and quantitative analysis of C₃F₈ and associated end products including CO₂, CO and CF₄ were carried out with FT-IR (Nicolet 6700, Thermo). The C₃F₈ removal efficiency is calculated by:

$$\text{C}_3\text{F}_8 \text{ removal efficiency} = \frac{[\text{C}_3\text{F}_8]_{\text{inlet}} - [\text{C}_3\text{F}_8]_{\text{outlet}}}{[\text{C}_3\text{F}_8]_{\text{inlet}}} \times 100\% \tag{1}$$

Here, [C₃F₈]_{inlet} and [C₃F₈]_{outlet} are the concentration of C₃F₈ at the inlet and the outlet of reactor, respectively. The selectivities of CO₂, CO and CF₄ are determined by:

$$\text{CO}_2 \text{ selectivity} = \frac{[\text{CO}_2]}{[\text{C}_3\text{F}_8]_{\text{inlet}} - [\text{C}_3\text{F}_8]_{\text{outlet}}} \times \frac{1}{3} \times 100\% \tag{2}$$

$$\text{CO selectivity} = \frac{[\text{CO}]}{[\text{C}_3\text{F}_8]_{\text{inlet}} - [\text{C}_3\text{F}_8]_{\text{outlet}}} \times \frac{1}{3} \times 100\% \tag{3}$$

$$\text{CF}_4 \text{ selectivity} = \frac{[\text{CF}_4]}{[\text{C}_3\text{F}_8]_{\text{inlet}} - [\text{C}_3\text{F}_8]_{\text{outlet}}} \times \frac{1}{3} \times 100\% \tag{4}$$

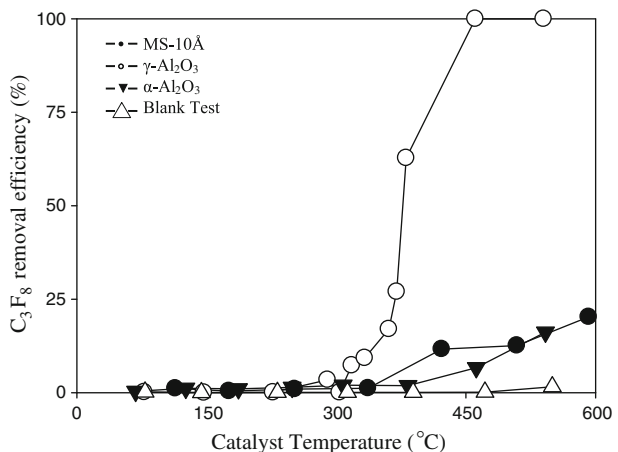
where [CO₂], [CO] and [CF₄] are the concentrations of CO₂, CO, and CF₄ at outlet of reactor, respectively.

Results and Discussion

Thermal Catalysis Test

The light-off curves for C₃F₈ removal achieved with molecular sieve (MS-10A) and aluminum oxide (γ-Al₂O₃, and α-Al₂O₃) are presented in Fig. 4. The blank test was carried out without packing. Apparently, MS-10A and α-Al₂O₃ do not have significant catalytic activity for C₃F₈ abatement while γ-Al₂O₃ starts showing catalytic activity at 300°C.

Fig. 4 Effect of catalytic activity on C₃F₈ removal efficiency. Gas compositions: C₃F₈ = 500 ppm, O₂ = 2%, and N₂ balance. Gas flow rate = 125 sccm



Adsorption Test

For all adsorption capacity tests, the adsorbent was packed in a glass tube with an inner diameter of 2.5 cm and the packing height was kept at 2.0 cm. The feeding gases contained 500 ppm C_3F_8 , 2% O_2 , and balanced N_2 . The gas flow rate, temperature, and pressure were controlled at 125 sccm, 25°C, and 1 atm, respectively. The adsorption capacity is determined by (5):

$$\begin{aligned} \text{Adsorption capacity (mg } C_3F_8/\text{g Adsorbent)} \\ = \frac{P \cdot (M.W.) \cdot Q \cdot 10^{-3}}{m \cdot R \cdot T} \int_0^t ([C_3F_8]_i - [C_3F_8]) dt \end{aligned} \quad (5)$$

where P is the pressure (atm), $M.W.$ is the molecular weight of C_3F_8 (g/mol), Q is the total gas flow rate (SLPM), m is the mass of adsorbent (g), R is the ideal gas constant (atm·L/mol·K), T is the gas temperature (K), t is the time required to reach adsorption saturation (min), and $[C_3F_8]_i$ and $[C_3F_8]$ are the inlet and outlet concentrations of C_3F_8 (ppm), respectively.

The adsorption capacities of molecular sieves (MS-3A, MS-4A, MS-5A, and MS-10A) and aluminum oxides ($\gamma\text{-Al}_2\text{O}_3$ and $\alpha\text{-Al}_2\text{O}_3$) for C_3F_8 are presented in Fig. 5. C_3F_8 adsorption capacity is in the order of MS-10A > MS-5A > MS-4A > MS-3A > $\gamma\text{-Al}_2\text{O}_3$ > $\alpha\text{-Al}_2\text{O}_3$.

In general, the BET surface area and average pore diameter are the important parameters in determining adsorption capacity, suggesting that it can be used as an indicator for selecting the appropriate adsorbent. Figure 6a and b shows the relationships between the BET surface area and average pore diameter and the adsorption capacity obtained with all the materials tested in this study. If one just focuses on the results obtained with molecular sieves, it seems that the adsorption capacity is strongly related to the average pore size. For instance, the average pore diameter of MS-3A, MS-4A, MS-5A and MS-10A are 3.52, 4.32, 5.2, 10.12 Å and the corresponding adsorption capacities are 0.92, 0.93, 0.98, 13.90 mg/g, respectively. Since the size of C_3F_8 molecule is 5.450 Å [11], the adsorption capacity should be low when the average pore size is smaller than 5.450 Å, which is

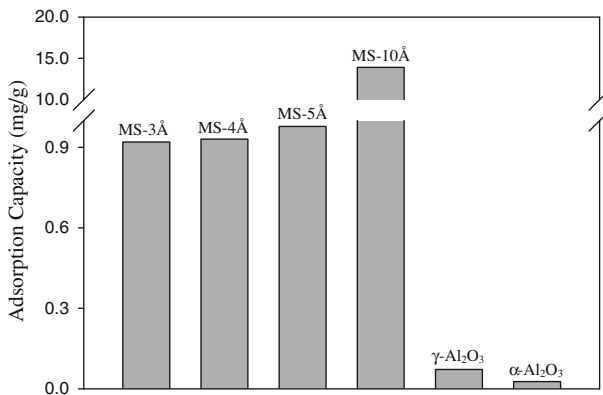


Fig. 5 Comparison of the adsorption capacities of various materials (MS-3A, MS-4A, MS-5A, MS-10A, $\gamma\text{-Al}_2\text{O}_3$, and $\alpha\text{-Al}_2\text{O}_3$) for C_3F_8

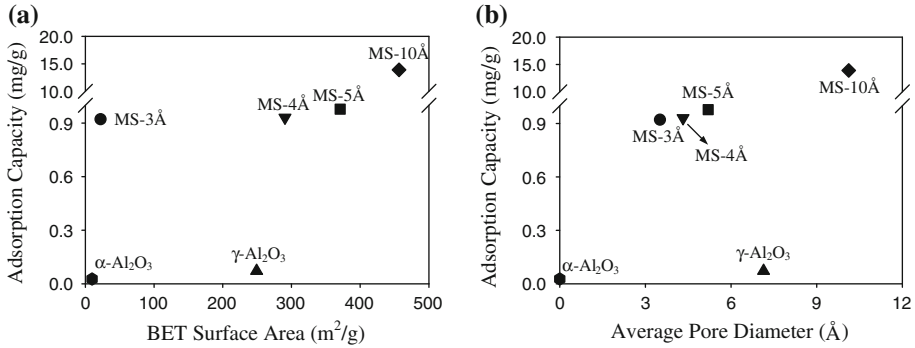
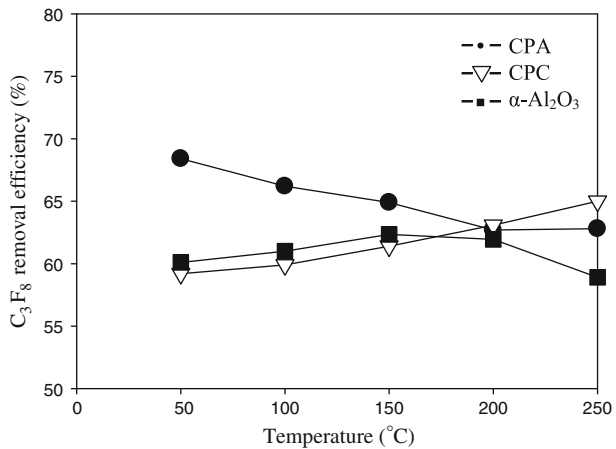


Fig. 6 Relationship between BET surface area (a) and average pore diameter (b) and C₃F₈ adsorption capacity for various materials tested in this study. Experimental conditions are the same as that described in Fig. 5

Fig. 7 Effect of operating temperature combined plasma with catalyst or adsorbent on C₃F₈ removal efficiency. Gas compositions: C₃F₈ = 500 ppm. O₂ = 2%, and N₂ balance. Gas flow rate = 50 sccm, discharge power = 20 W



consistent with the experimental results. However, it needs to be emphasized that the average pore size seems not the only factor dominating the adsorption capacity. For instance, the average pore size of γ -Al₂O₃ is actually greater than the molecule size of C₃F₈, however, the adsorption capacity for C₃F₈ is still insignificant. Further study on this topic is needed to establish a suitable indicator to provide useful information for the selection of an appropriate adsorbent.

Comparison of C₃F₈ Abatement Via CPC, CPA and CPACs

γ -Al₂O₃ and MS-10A are selected for the experimental tests for CPC and CPA because of their good adsorption capacity and catalytic activity for C₃F₈, respectively. The dependence of C₃F₈ removal efficiency on the operating temperature of the system combining plasma with catalyst or adsorbent is presented in Fig. 7.

As shown in Fig. 7, the performance of CPA is better than that of CPC when the operating temperature is between 50 and 150°C. The C₃F₈ removal efficiencies of α -Al₂O₃ and CPC were almost the same, suggesting that catalysis is ineffective for C₃F₈ abatement

at this temperature window. The reason is mainly attributed to the low activity of catalysts when the temperature is controlled at the range of 50–150°C. On the contrary, CPC could achieve better performance instead as the temperature is raised to 250°C. Higher C_3F_8 removal efficiency achieved with CPC results from the higher activity of catalysts. The C_3F_8 removal efficiency of CPA decreases with increasing operating temperature because higher temperature is unfavorable for physical adsorption.

In order to combine the advantages of the two types of packing materials tested in this study, the co-operation of adsorption and catalysis was studied. MS-10A was mainly applied to enhance the adsorption, whereas $\gamma-Al_2O_3$ was used as the catalytically active component. The combination was realized by introducing the same volumes of adsorbent and catalyst in the arrangement of separate layers (A/C layer or C/A layer) or a layer of mechanical mixture (A/C mixture). Here, A/C layer represents the adsorbent is placed upstream of the catalyst while C/A layer stands for the location of catalyst is ahead of adsorbent.

Dependence of C_3F_8 removal efficiency on the operating temperature achieved with CPACs with different configurations is presented in Fig. 8. When the operating temperature is below 150°C, the performance of C_3F_8 abatement is in the order of A/C layer \approx A/C mixture > C/A layer at a fixed temperature. The purpose of packing adsorbent within the plasma reactor is to increase C_3F_8 concentration and retention time in the discharge zone. In the configuration of C/A layer, C_3F_8 is immediately adsorbed once the gas stream enters the plasma reactor. Therefore, compared with CPAC (C/A layer), it can be expected that the probability of the collision between C_3F_8 and the active species generated in plasma would be higher in CPAC (A/C layer). As for CPAC (A/C mixture), it can be considered that half of the adsorbent is placed in the first of the plasma reactor with the assumption that adsorbent and catalyst are homogeneously mixed. As a result, it is not surprising that CPAC (A/C mixture) achieved better performance than CPAC (C/A layer). Nevertheless, it needs to be noticed the differences between the C_3F_8 removal efficiencies achieved with different CPACs are less significant as the temperature is increased.

On the other hand, by comparing the results presented in Figs. 7 and 8, it can be concluded that C_3F_8 removal efficiencies obtained with different plasma reactors are in the order as: CPAC (A/C layer; AC mixture) > CPA (plasma with adsorbent alone) > CPC

Fig. 8 Effect of the packing way (single-component layers and mechanical mixture) on C_3F_8 removal efficiency. Gas compositions: $C_3F_8 = 500$ ppm, $O_2 = 2\%$, and N_2 balance. Gas flow rate = 50 sccm, discharge power = 20 W

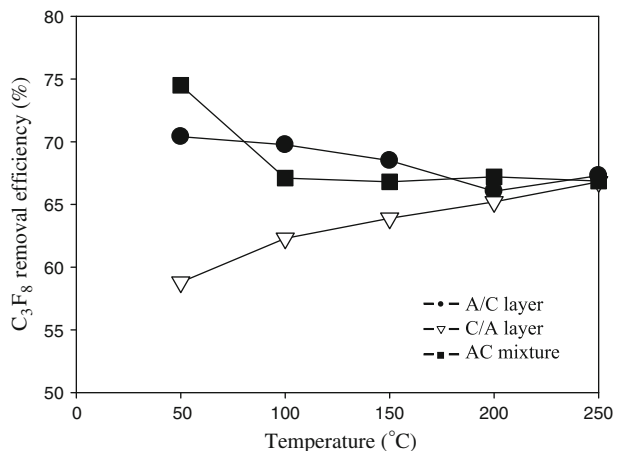
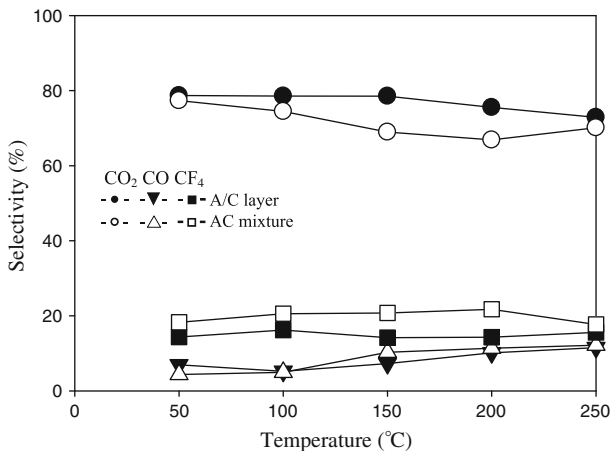


Fig. 9 Comparison of the selectivities of CO_2 , CO , and CF_4 achieved with different CPACs. Gas compositions: $\text{C}_3\text{F}_8 = 500$ ppm, $\text{O}_2 = 2\%$, and N_2 balance. Gas flow rate = 50 sccm, discharge power = 20 W



(plasma with catalyst alone) > CPAC (C/A layer), confirming the benefits of the simultaneous combination of adsorption, catalysis and plasma for C_3F_8 removal.

Products Selectivity and Carbon Balance

The products' selectivities obtained with CPACs (A/C layer and AC mixture) are shown in Fig. 9. The major end products identified by FT-IR include CO_2 , CO , N_2O and CF_4 . The concentrations of N_2O ranged from 150 to 300 ppm, depending on the reactor configuration and operating temperature. Moreover, it is worth noticing that both NO and NO_2 are not detected in this study; however, the reasons for this interesting phenomenon is still unclear and further study is needed. The carbon balance ranges from 95 to 100%, meaning that most of the carbon from C_3F_8 removal has been transformed to CO_2 , CO , and CF_4 . Furthermore, it needs to be emphasized that the formation of C_2F_6 is not observed in this study, indicating that the novel technique proposed is promising for C_3F_8 abatement in that the GWP of C_2F_6 is higher than that of C_3F_8 .

Conclusions

Several novel plasma reactors, including CPC, CPA and CPACs (A/C layer, C/A layer and A/C mixture) are experimentally tested for C_3F_8 abatement in this study. The dependences of C_3F_8 removal efficiencies obtained with CPC and CPA on the temperature are completely different. For CPC, increasing temperature is beneficial for C_3F_8 decomposition due to the increased catalytic activity. On the contrary, increasing temperature is unfavorable for C_3F_8 abatement in CPA because higher temperature would result in a lower adsorption capacity. Moreover, the experimental results show that CPAC could achieve better performance than CPC and CPA. However, one must be careful in choosing the right configuration. For example, CPAC (C/A layer) would lead to poorer performance compared with CPC and CPA. On the other hand, it needs to be mentioned that the global warming potential of C_2F_6 is actually higher than that of C_3F_8 . Therefore, the plasma treatment would be meaningless if most of the C_3F_8 molecules decomposed are converted into C_2F_6 . Fortunately, the generation of C_2F_6 is not observed in this study, suggesting the feasibility of C_3F_8 abatement via CPAC.

Acknowledgments The authors gratefully acknowledge the financial support provided by Industrial Technology Research Institute of Taiwan (grant number 985914).

References

1. Holzer F, Roland U, Kopinke F-D (2002) Combining of nonthermal plasma and heterogeneous catalysis for oxidation of volatile organic compounds Part 1. Accessibility of the intra-particle volume. *Appl Catal B-Environ* 38:163–181
2. Kim HH, Ogata A, Futamura S (2006) Effect of different catalysts on the decomposition of VOCs using flow-type plasma-driven catalysis. *IEEE Trans Plasma Sci* 34:984–995
3. Kim HH (2004) Nonthermal plasma processing for air-pollution control: A historical review, current issues, and future prospects. *Plasma Process Polym* 1:91–100
4. Chang MB, Lee HM (2004) Abatement of perfluorocarbons with combined plasma catalysis in atmospheric-pressure environment. *Catal Today* 89:109–115
5. Magureanu M, Mandache NB, Gaigneaux E, Panu C, Parvulescu VI (2006) Toluene oxidation in a plasma-catalytic system. *J Appl Phys* 99:123301
6. Chavadej S, Saktrakool K, Rangsunvigit P, Lobban LL, Sreethawong T (2007) Oxidation of ethylene by a multistage corona discharge system in the absence and presence of Pt/TiO₂. *Chem Eng J* 132:345–353
7. Subrahmanyam Ch, Magureanu M, Renken A, Kiwi-Minsker L (2006) Catalytic abatement of volatile compounds assisted by non-thermal plasma Part 1. A novel dielectric barrier discharge reactor containing catalytic electrode. *Appl Catal B Environ* 65:150–156
8. Harling AM, Demidyuk V, Fischer SJ, Whitehead JC (2008) Plasma-catalysis destruction of aromatics for environmental clean-up: Effect of temperature and configuration. *Appl Catal B-Environ* 82:180–189
9. Chen HL, Lee HM, Chen SH, Chang MB, Yu SJ, Li SN (2009) Removal of volatile organic compounds (VOCs) by single-stage and two-stage plasma catalysis systems: a review of the performance enhancement mechanisms, current status and suitable applications. *Environ Sci Technol* 43:2216–2227
10. Manley TC (1943) The electrical characteristic of the ozonator discharge. *Trans Electrochem Soc* 52:5820–5828
11. Gindulytė A, Mass L, Banks BA, Miller SKR (2002) Direct C-C bond breaking in the reaction of O (3P) with fluoropolymers in low earth orbit. *J Phys Chem A* 106:5463–5467